Journal of Marine Science and Technology

Volume 27 | Issue 4 Article 5

PROTECTIVE EFFECT OF AN ICE-BREAKING STRUCTURE ON OFFSHORE STRUCTURES IN SHALLOW WATERS

Ji-Wu Dong
Department of architectural and civil engineering, Hefei University, Hefei, China. Water Science and Water Disaster Prevention and Control in Hunan Province Key Laboratory, Changsha University of Technology, Changsha, China. State Key Laboratory of Coastal and Offshore Engineering, Dalian University of Technology, Dalian, China. 4 College of Environmental Science and Engineering, Dalian Maritime University, Dalian, China., jiwudong@dlut.edu.cn

Zhi-Jun Li
State Key Laboratory of Coastal and Offshore Engineering, Dalian University of Technology, Dalian, China

Xiang-Peng Kong
College of Environmental Science and Engineering, Dalian Maritime University, Dalian, China.

Xiao-Dong Liang
Department of architectural and civil engineering, Hefei University, Hefei, China

PROTECTIVE EFFECT OF AN ICE-BREAKING STRUCTURE ON OFFSHORE STRUCTURES IN SHALLOW WATERS

Acknowledgements

The authors are very grateful to the Key Project of Natural Science in Colleges and Universities in Anhui Province (No. KJ2015A175, No. KJ2018A0558); the Key Laboratory of Water-Sediment Sciences and Water Disaster Prevention of Hunan Province (No. 2015SS06); the Key Project of Visiting Domestic and Overseas of Outstanding Youth Core Talents of Colleges and Universities in Anhui Province (No. gxfxZD2016218); the Key Program of the National Natural Science Foundation of China (No. 51639003); the Scientific Research Fund Project of Talents of Hefei University (No. 14RC01); the Talent Research Fund Project of Hefei University (No. 16-17RC02).

Journal of Marine Science and Technology, Vol. 27, No. 4, pp. 343-351 (2019)
DOI: 10.6119/JMST.201908_27(4).0005

PROTECTIVE EFFECT OF AN ICE-BREAKING STRUCTURE ON OFFSHORE STRUCTURES IN SHALLOW WATERS

Ji-Wu Dong[1,2,3], Zhi-Jun Li[3], Xiang-Peng Kong[4], and Xiao-Dong Liang[1]

Key words: sea ice, model test, protective effect, shallow water area.

ABSTRACT

In this study, an ice-breaking structure (IBS) was designed to break large ice floes into small fragments through flexural failure predominantly for protecting offshore structures in shallow waters. The protective effect of the IBS on a vertical isolated cylindrical pile (ICP), which was examined through the model tests of the crushing ice loads and collision forces on the ICP from ice pieces broken with the IBS under identical conditions, was evaluated by obtaining the relative difference between the maximum values of the horizontal crushing forces and collision loads on the ICP. The results indicated a notable protective effect of the IBS on the ICP. Moreover, the ice load against the ICP was reduced by approximately 80% when the waterline was not higher than 0.8 times the height of the IBS. The protective effect of the IBS was primarily influenced by the relative water level and was less affected by the relative distances between the two structures. Ice pile-up and ride-up tests on the IBS with a sloping artificial island (SAI) at the downstream indicated that the IBS had an appreciable shelter effect on the SAI. When the water level higher than 0.93 times height of the IBS, the shelter effect of the IBS on the SAI was approximately 4.3, which was measured using the ratio of the height of the ice rubble to the height of the IBS.

I. INTRODUCTION

Offshore structures, particularly vertical structures in icy waters, may experience extremely high loads without ice mitigation strategies. With the development of the oil and gas industry, the safety of offshore structures and the design of ice protection structures have received considerable research attention. The ice load of crushing failure is approximately six times that of flexural failure when the other parameters are equal (Timco and Johnston, 2004). This observation indicates that structures with sloping sides (upward or downward) or curves withstand lower ice actions than structures with vertical sides. Therefore, offshore structures in shallow areas are equipped with ice-breaking structures (IBSs) having sloping sides (upward or downward) or curves. Ice-breaking cones (or similar cone-shaped structures) commonly used in the Bohai Sea on jacket oil platforms generally comprise upward and downward breaking cones (Wang et al., 2015). Similar ice-breaking cones are found in other waters. Offshore wind turbines are equipped with downward IBSs in the Baltic Sea (Shi et al., 2016). Upward-breaking cones are used in the Confederation Bridge of Canada (Brown and Määttänen, 2009). The cones are advantageous for reducing ice loads and ice-induced vibrations against vertical offshore structures. However, vibrations can still be easily observed from compliant jacket platforms with ice-breaking cones when drifting ice moves at a high speed. These vibrations affect offshore platform operations, cause fatigue, and degrade platform performance (Yue and Bi, 2000). Because periodical ice forces, which are related to the breaking length and ice speed, are still observed on jacket platforms, although the dominant ice failure mode is transformed from crushing to bending or buckling. Zhang and Yue (2011) attributed this observation to the dominant frequency of ice actions being close to the natural frequency of platforms. Therefore, it is necessary for the jacket platforms with ice cones to be optimized by improving the ice-induced fatigue of tubular joints (Li et al., 2008). Isolation cones in the jacket platform with springs and dampers can be useful to minimize ice-induced vibrations (Wang et al., 2013).

Because ice rubbles are significant in load reduction on offshore structures (Timco, 1990; Liferov and Bonnemaire, 2005; Liferov, 2005), several ice barriers of ice rubble generators (IRGs) and ice protection structures (IPSs) (Jochmann et

Paper submitted 03/11/19; revised 05/06/19; accepted 06/12/19. Author for correspondence: Ji-Wu Dong (e-mail: jiwudong@dlut.edu.cn).
[1] Department of architectural and civil engineering, Hefei University, Hefei, China.
[2] Water Science and Water Disaster Prevention and Control in Hunan Province Key Laboratory, Changsha University of Technology, Changsha, China.
[3] State Key Laboratory of Coastal and Offshore Engineering, Dalian University of Technology, Dalian, China.
[4] College of Environmental Science and Engineering, Dalian Maritime University, Dalian, China.

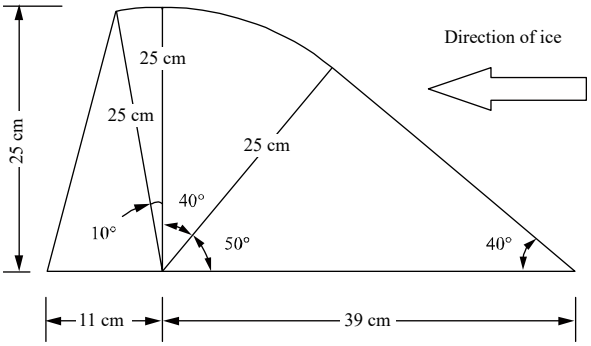

Fig. 1. Schematic of the IBS model for evaluating the protective effect on the ICP.

al., 2003; Gürtner and Berger, 2006) have been proposed to minimize ice forces on offshore structures in shallow icy waters, such as the Caspian Sea and Great Lakes. IRGs and IPSs with inclined planes, curved surfaces, several vertical piles, or piles having steep obliquity (Barker and Timco, 2005), are generally employed to prevent ice floes from colliding with sheltered structures or to generate ice rubbles for protecting downstream structures. Evers and Weihrauch (2004) asserted that ice barriers of barges equipped with piles and a light-weight ice barrier with an inclined roof structure mounted on a barge are the two optimal IRGs for shallow icy waters. However, vertical piles or piles with steep obliquity withstand strong ice crushing forces. Thus, piles must be sufficiently strong, which may increase the cost. Furthermore, ice barriers with inclined roof structures must be anchored at the sea bottom with highly difficult construction.

This approach of isolating an IBS from the protected structures has some advantages. The IBSs must have an ideal stability with low loadings. Therefore, IBSs with heavy gravity are suitable for shallow waters. Gürtner (2009) examined a gravity-type structure named shoulder ice barrier (SIB) for shallow waters with a high vertical force and an inclination angle of 30° to induce ice failure in bending. The SIB was designed to prevent ice sheets from over-riding the structure. However, there is a negligible effect on the SIB against the protected structure when the distance between the two structures is sufficiently large regardless of the occurrence of ice pile-up and ride-up. When ice pieces run over the SIB, the loading on the downstream structures is still considerably low because of the small sizes of the fragments.

The heavy forces on offshore structures always arise from the large-sized floating ice. Thus, this study focused on the breaking ice sheets in bending failure caused by an IBS. The IBS comprises an inclined plane and a circular surface oriented toward the floating ice (Fig. 1). This structure was proposed for applications in northern Bohai Sea and other shallow water areas. The sloping and curved surfaces were designed to break level ice under bending or buckling failure by exerting low ice forces on them. The curved surface of the structure facilitated the riding-up of ice fragments at high water levels. The wedge shape at its back improved structural stability. The crushing failure or mixed mode failure with crushing and flexure was dominant for a high inclination angle (e.g., larger than 60°) of the inclined plane. Furthermore, a high inclination angle increased the ice forces on the IBS and decreased its stability under ice actions. Consequently, the largest angle applied for the IBS was 40°.

Table 1. Parameters of the model ice.

Thickness (mm)	Compressive strength (kPa)	Flexural strength (kPa)	Elastic modulus (MPa)
12.5	71	68	15
13	73	63	66
13	77	84	37
17	92	89	20
19	78	74	53
19.5	94	89	37

This study aimed to examine the shelter effect of the IBS on vertical offshore structures represented using a vertical isolated cylindrical pile (ICP) model. The differences between the crushing forces from the level ice and ice fragments on the ICP were compared to demonstrate the ice load reduction for evaluating the protective effect of the IBS on the ICP. The factors influencing the protective effect are also discussed. Barker and Timco (2016) stated that ice pile-up always occurs at a suitable water level in the presence of an obstacle. Therefore, the IBS can be used as an IRG to shelter the structures behind it. An accident that occurred at the end of 2005 and was caused by floating ice was investigated in northern Bohai Sea (Kong and Chen, 2013). The ice had a thickness of 30 cm over a wave wall and a height of 1.2 m along the slope of an artificial island that interrupted oil production. A sloping artificial island (SAI) model was used to examine the protection of the IBS against sloping structures by simulating ice pile-ups and ride-ups on the IBS.

II. PHYSICAL MODEL TESTS

Physical model tests were conducted in a flume in the State Key Laboratory of Coastal and Offshore Engineering, Dalian University of Technology. The towing carriage in the flume was used to move the ice sheet at a constant velocity of 10 cm/s in a straight line. DUT-1 nonrefrigerated model ice was used for the tests. The ice is a composite of polypropylene powder, plastic particles, cement, water, and other materials, as validated in previous studies (e.g., Li et al., 2002; Dong et al., 2012). The primary parameters of the model ice have been studied (e.g., Li et al., 2001; Li et al., 2003), and its typical flexural strength and compressive strength are 20-75 and 20-150 kPa, respectively. The coefficients of kinetic friction for ice on ice, concrete, and synthetic glass are approximately 0.49, 0.41, and 0.32, respectively. The high kinetic friction coefficients of the model ice on several types of materials are

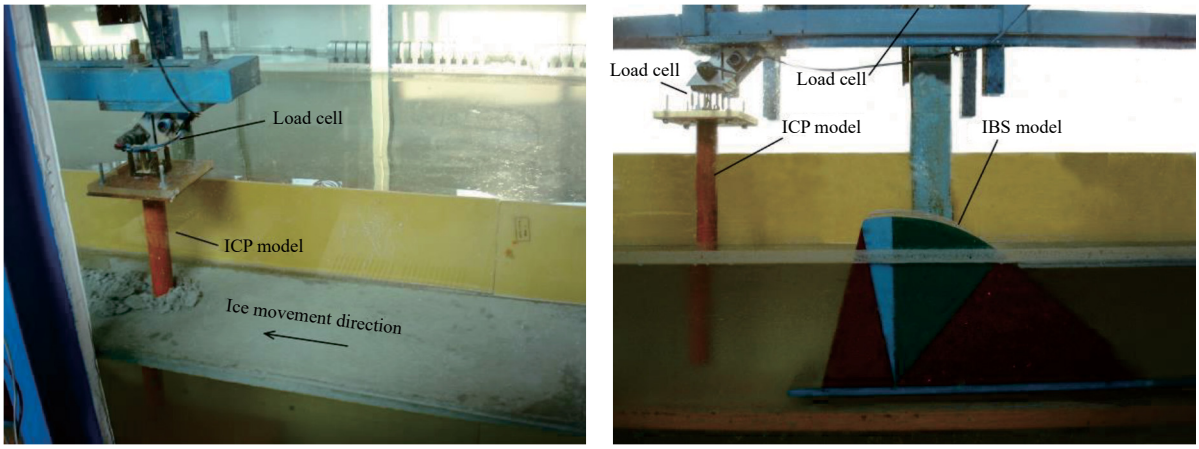

(a) (b)

Fig. 2. Setup for measuring the horizontal crushing ice loads on the ICP (a) (The IBS is at the downstream, not in the photo) and the horizontal ice forces on the IBS and impact forces on the ICP from the ice pieces (b).

(a) (b)

Fig. 3. Ice failure on the IBS at different water levels. Pile-up occurs upstream at the low water level (a). Ice ride-up on the IBS and its impact on the ICP at the high water level (b).

attributed to its grain structure and rough surface. The density of the model ice is 880-920 kg/m^3.

1. Tests of the Protective Effect of the IBS on the ICP

Although sheets of the DUT-1 model ice are made in molds of the same size, differences are primarily observed in the mechanical characteristics because manual work is required in the manufacturing process. To reduce the artificial error and to compare the loads on the ICP with and without upstream IBS under the same conditions, an electric drilling machine was used to cut each ice sheet into three identical parts with a width of 26 cm. Table 1 presents the parameters of the DUT-1 model ice in the tests. Model ice with five different thicknesses in the range of 12.5-19.5 mm were adopted to evaluate the effect of physical and mechanical factors on the lengths of broken blocks and the horizontal forces on the IBS. The IBS and ICP models comprised synthetic glass with a height of 25 cm and a straight thin-wall steel pile with a diameter of 32 mm.

The crushing ice forces on the ICP [Fig. 2(a)], impact forces exerted by the ice pieces, and horizontal force on the IBS were measured. The upstream ice pieces were cleaned after measuring the crushing ice loads on the ICP, and the pieces were then moved to the back of the IBS. Therefore, the impact forces on the ICP and the horizontal ice force on the IBS could be measured, all else being equal [Fig. 2(b)]. The IBS model was fixed with a biaxial force sensor having a sampling rate of 100 Hz, and the ICP with a load cell having the same sampling rate was fixed on a steel plate with protuberances on its two sides. The IBS and ICP were fixed on a channel steel structure at an interval of 5 cm between several grooves at the bottom. With the protuberance biting the grooves, the ICP with load cell was fixed using two screws on the channel steel structure. In this manner, the ICP could be easily slid from the front to the back of the IBS. The distance between the two structures could be easily regulated by moving the ICP along the grooves in the channel steel structure. Moreover, a 4-m-long board was placed parallel to the side wall of the flume, and the distance between these two structures was approximately 6 cm wider than the width of the IBS. Therefore, ice sheets acted against the IBS and ICP along a line. According to (Lu et al., 2014), the IBS is a "wide-sloping structure." Thus, a two-dimensional (2D) model can be used to describe the interaction between the ice and IBS.

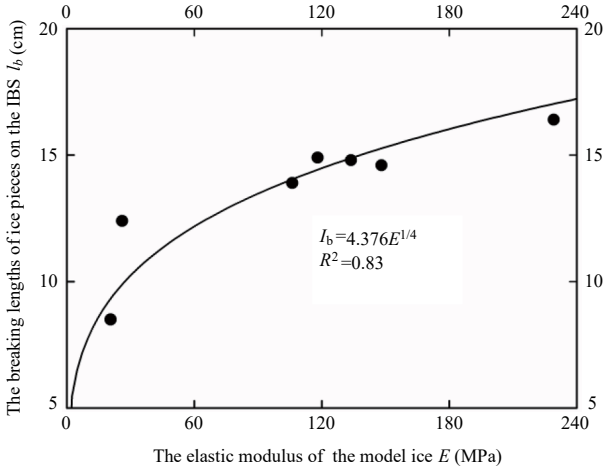

Fig. 4. Relation between the elastic modulus and the mean length of the ice fragments.

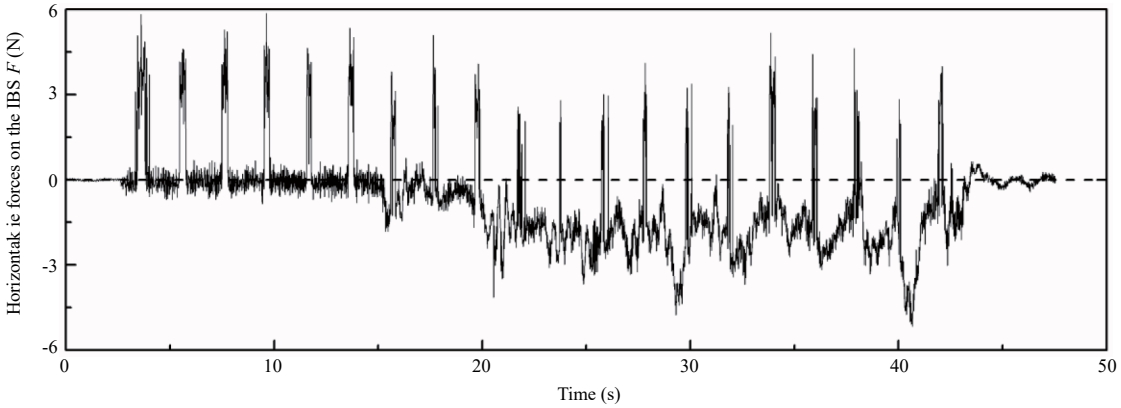

Fig. 5. Variation in the horizontal ice forces on the IBS with time.

2. Tests of the Protective Effect of the IBS on the SAI

The SAI model had a gradient of 1: 2 and a height of 12 cm (excluding the 4-cm wave wall). The size of the model was 1/30th the size of the artificial island in northern Bohai Sea. The distance between the foot of the SAI and the lowest point at the back of the IBS was 1 m. The sizes of the two models were decreased to reduce the ice mass to minimize costs. A solid concrete IBS model with a height of 12.5 cm was prepared, which was half the size of the synthetic glass IBS model. The width of the DUT-1 model ice was reduced twice, and its thickness was 10 mm. Tests were conducted according to the constraints of the board and sidewall of the flume, and a foundation with a height of 10 cm at the bottom of the IBS was adopted for the convenient viewing of ice ride-up and pile-up at a low water level.

III. RESULTS

1. Ice Failure Modes with Different Waters and Ice-Breaking Lengths in Varying Ice Elastic Modulus

When the water depth was lower than the topside of the IBS, the ice primarily broke with an upward-flexural failure. The lengths of the broken ice fragments were small, and grounded ice rubble formed upstream at a low water level. This behavior was attributed to the multiple interactions between the broken fragments and moving ice sheets. Because of a high freeboard, the broken pieces rarely crossed the IBS; however, they slid down at its foot [Fig. 3(a)]. Downward-bending failure of the ice occurred when the broken pieces converged and gradually formed an ice rubble, which hindered the ride-up of ice sheets on the IBS. Therefore, the structures behind the IBS were sheltered. The rise in the water level, particularly over the boundary between the plane and curved surface of the IBS, resulted in a low angle at the waterline and large lengths of the fragments [Fig. 3(b)]. At this time, ride-up was likely to occur and an ice rubble appeared downstream. Furthermore, the forces on the ICP increased, due to which a minimized protecting effect of the IBS was observed on the ICP under the aforementioned circumstances. The IBS withstood decreased forces with a rising water level.

The ice-breaking lengths were measured in the test of the protective effect of the IBS against the ICP. One ice block was measured three times in the ice movement direction. The

Table 2 Test results for β, φ and δ.

Run #	β	φ	δ
1	0.43	1.02	0.89
2	0.43	1.92	0.91
3	0.77	0.91	0.92
4	0.77	1.05	0.86
5	0.77	1.78	0.81
6	0.77	1.78	0.87
7	0.77	1.30	0.76
8	0.77	1.98	0.94
9	0.87	1.01	0.65
10	0.87	1.32	0.72
11	0.87	1.42	0.89
12	0.91	1.54	0.91
13	0.91	1.63	0.77
14	0.91	1.67	0.76
15	1.03	1.80	0.12
16	1.03	1.29	0.09
17	1.07	NA	0.00

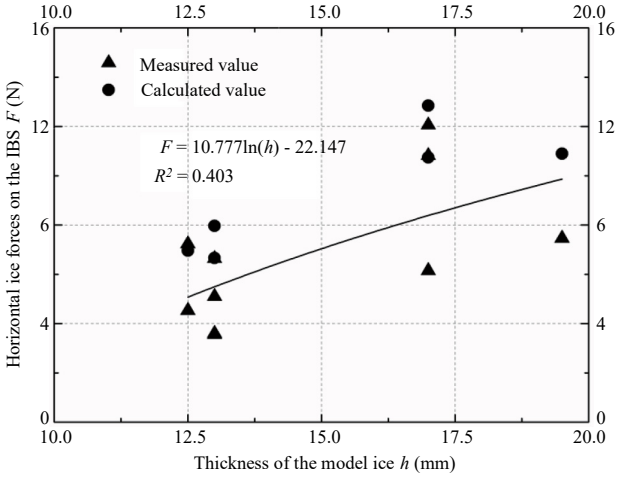

Fig. 6. Horizontal ice forces on the IBS of model ice with different thicknesses.

measurements were conducted from the two endpoints and midpoint of its width, and the average value was used as the breaking length. The ice pieces that broke twice because of collision with the ICP and interaction with each other were not included. To avoid the effect of ice failure modes on the lengths of ice pieces, ice blocks with a waterline not higher than the boundary between the plane and curved surfaces of the IBS were analyzed.

The lengths of the ice pieces were 10-30 cm, which increased with increasing ice thickness. The fragments had a relatively high length, which was approximately 10 times the ice thickness. The results indicate that the mean lengths of the broken ice blocks increased with increasing ice elastic modulus (Fig. 4). Although a high cement content in the DUT-1

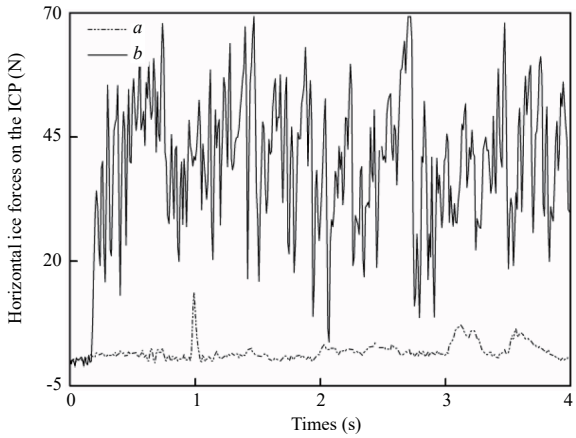

Fig. 7. Comparison of the ice crushing and impact forces on the ICP: (a) variation in the impact ice forces with time and (b) variation in the crushing ice forces with time.

model ice caused the broken pieces with high lengths, a protection effect of the IBS against the ICP was observed because of the bending failure at the high or low water level.

2. Horizontal Ice Forces on the IBS and the Affecting Factor of Ice Thickness

The time series displayed in Fig. 5 indicates the test results for the variations in the horizontal ice loads against the IBS. The lateral forces on the IBS increased from approximately zero as the ice sheets failed in upward bending failure. The lateral forces decreased rapidly at the end of the failure within approximately 0.2 s. A similar periodicity was observed for the changes in loads at intervals of approximately 2 s. The ice thickness was 12.5 mm and the distance between the IBS and ICP was 19.8 cm. The water level (from the bottom of the IBS) was 19.2 cm, which was at the borderline between the curved surface and inclined plane. The average and maximum values of the peak loads (horizontal loads against the IBS) were 5.3 and 5.9 N, respectively (Fig. 5). By contrast, the peak load was 40 N for the crushing force on the ICP from the same strip of the ice sheet. Thus, the IBS could withstand a small force as an ice protecting structure. A negative value of horizontal forces on the IBS could be observed from the plot, particularly after approximately 15 s. After riding-up, the ice blocks were confined to a relatively small space. Consequently, they collided with each other between the two structures. Some of the fragments exhibited an inclined action against the IBS [Fig. 3(b)]. If the waterline was not higher than the borderline, the maximum horizontal force against the IBS was generally invariable when the other parameters were equal because of the unchanged oblique angle for the slope plane. Fig. 6 illustrates the loads on the IBS of five different ice thicknesses when the water level was not higher than the borderline. The trend of an increase in forces with increasing ice thickness was not prominent. The theoretical 2D model described in (Croasdale and Cammaert, 1994) was used to calculate the theoretical loads on the IBS, which were marginally higher

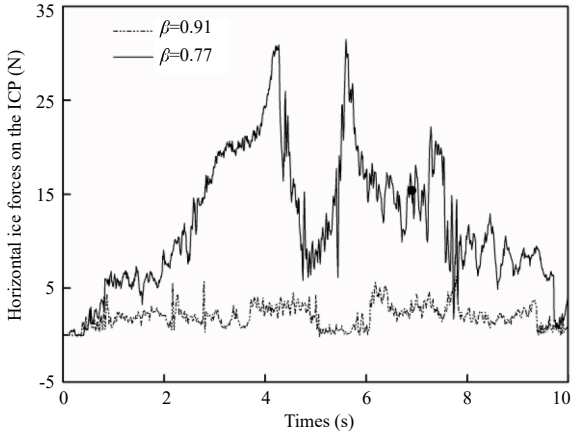

Fig. 8. Impact forces on the ICP with different relative water levels (φ = 2).

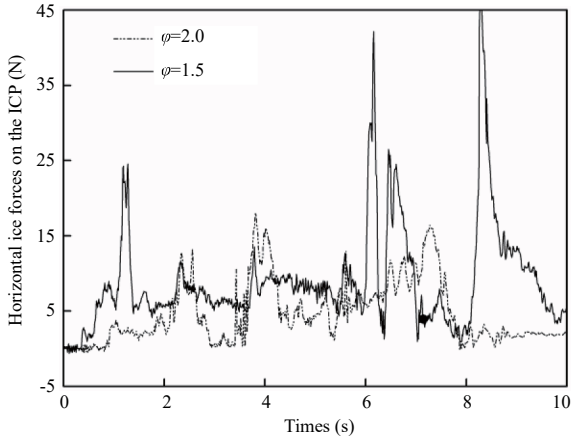

Fig. 9. Impact forces on the ICP for different relative distances (β = 0.87).

than the measured loads. The maximum load of all the data points was approximately 12.1 N. The IBS was suitable for a protecting structure withstanding low force with a high stability.

3. Contrast Between the Ice Crushing and Impact Load on the ICP

Fig. 7(a) illustrates the impact forces of the ice pieces on the ICP, which was protected by the IBS and had a peak load of approximately 14 N. With 12.5-mm-thick model ice, the waterline was at 19.2 cm from the bottom of the IBS. The compressive strength and flexural strength of ice were 72.89 and 62.59 kPa, respectively. Fig. 7(b) displays the crushing ice force on the ICP under identical experimental conditions typically encountered in the tests, with a peak crushing force of approximately 70 N. The significant shelter effect of the IBS on the ICP was observed by comparing the two plots. A complex loading of ice pieces was observed, where some of the pieces rotated and collided with each other before acting on the ICP after overtopping the IBS. However, the ICP behind

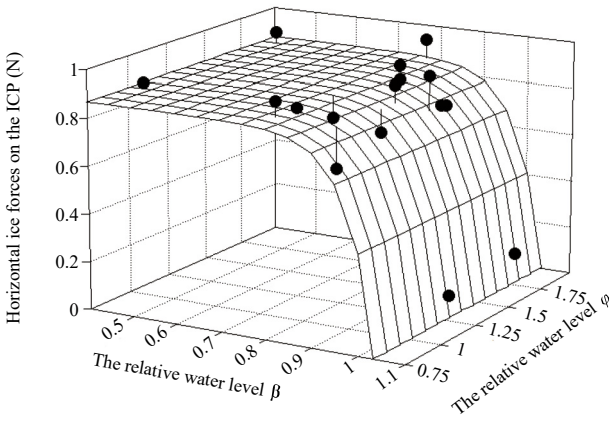

Fig. 10. Correlation between the index of ice force reduction (δ), relative distance (φ), and relative water level (β).

the IBS was subjected to a low force primarily because of the small size of the ice blocks resulting from flexural failure.

4. Magnitude and Factors Influencing the Shelter Effect of the IBS on the ICP

To quantify the protective effect of the IBS on the ICP, the index δ of the relative value of force reduction was defined for the tests as follows:

$$\delta = \left(F_1 - F_2\right) / F_1 \tag{1}$$

where F_1 and F_2 are the maximum values of the horizontal crushing forces and collision loads on the ICP caused by ice fragments under identical conditions, respectively. Further more, the nondimensional parameter β, which denotes the relative depth, is defined using the ratio of the water level from the bottom of the IBS to its height. The value of β was 0.77 when the waterline was at the boundary between the plane and curved surfaces. The relative distance φ was defined as the ratio of the distance between the ICP and IBS at the water level to the lengths of the ice pieces. Table 2 presents the test results. When the relative water level β increased to 1.07, the IBS became ineffective. The value of δ was not equal to zero when β was 1.03. One of the reasons for this result was the effect of the ice thickness. There still existed a possibility that the ice sheets could affect the IBS and cause flexural failure. Therefore, β had a negligible effect on the ICP when it approximated to 1.

The value of δ was primarily of the order of 0.8, and δ varied with β and φ when the ice thickness and other factors were unchanged. The results indicated that the effect of β on δ was particularly remarkable for a β value higher than 0.77. When β decreased from 0.91 to 0.77, δ increased from 0.7 to 0.87 (φ = 1.98, Fig. 8). The decrease in β increased the freeboard height of the ice fragments and the tilt of the IBS at the waterline, which resulted in the generation of small ice fragments. Therefore, a decrease in the kinetic energy of the fragments and impact forces on the ICP increased δ. When β

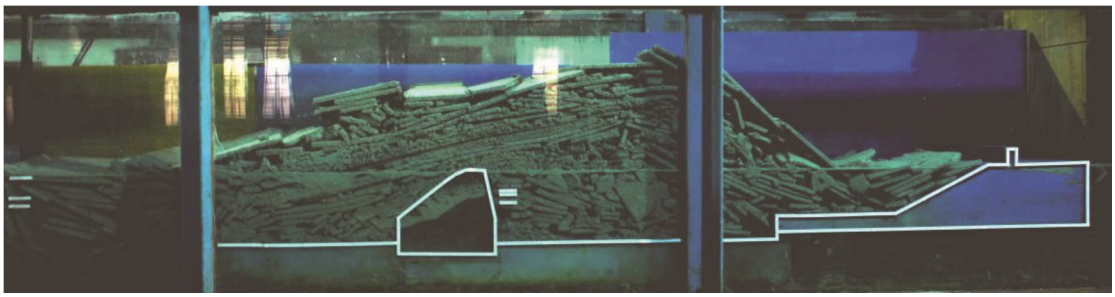

Fig. 11. Maximum height of the ice rubble.

Fig. 12. A new rubble on the sloping surface of the original rubble.

was lower than 0.77, the ice fragments accumulated and formed an ice rubble because a majority of the fragments could not ride-up the IBS. Therefore, few fragments affected the ICP. Therefore, with a decrease in β (< 0.77), δ gradually reached a maximum value of 1.

Fig. 9 indicates that φ had an evident effect on δ. When β was 0.87, φ increased from 1.5 to 2 and δ decreased by 0.23. However, the effect of φ on δ was not noticeable in most cases. Fig. 9 displays high peak pulses at the end of the time series of φ = 1.5. This is due to a broken block with a higher length, which obliquely impacted the ICP in the upward direction. Irregular collision of the fragments resulted in abnormal actions on the ICP, which were different from crushing loading. The unchanged β resulted in an invariant angle at the waterline and a constant average length of the ice pieces. The broken blocks moved a long distance and lost a large amount of kinetic energy before colliding with the ICP, which was attributed to the increasing φ. A small impact force on the ICP was observed for a sufficiently large φ. The kinetic energy of the ice pieces was considerably reduced because of the reduction in their sizes caused by bending failure. The fluid velocity at the back of the IBS was approximately equal to 0. Therefore, the process of broken pieces falling into water, overcoming the drag force of static water, and interacting with each other required a considerable amount of energy. Therefore, φ had a smaller effect on δ than β did. In general, very small forces, which is not appreciably affected by φ, are exerted on the ICP by broken fragments.

The data in Table 2 were used to plot a wire-mesh surface (Fig. 10). The surface had a similar shape to the IBS. Although the data were considerably scattered, a trend can be seen in the plot. δ was higher than 0.8, particularly for a β lower than 0.8. Therefore, the protective effect of the IBS against the ICP was remarkable. Under the aforementioned conditions, the ice loads against the ICP could be reduced by approximately 80%. By contrast, δ was significantly reduced from 0.8 to approximately 0 for a β value higher than 0.8. The plot in Fig. 10 indicates that φ had a small effect on δ.

5. Protection Effect of the IBS Against the SAI

An ice rubble with small lengths of ice pieces was observed upstream for a β value of 0.16 because of the high freeboard. Ride-up on the IBS was observed when β was increased to 0.48. The maximum rubble height was 53.6 cm, and the ice pieces did not reach the wave wall (Fig. 11). Several broken ice blocks were observed on the sloping plane of the SAI, with a majority of the remaining pieces accumulated above the IBS. The ratio of the maximum heights of the rubble to the height of the IBS was used to quantify the protection effect of the IBS on the SAI, which reached an appreciable value of 4.3 for a β

value of 0.93.

The pile-up height did not increase further beyond a certain value. A new ice pile appeared on the existing pile and was oriented toward the ice movement (Fig. 12). Barker and Croasdale (2004) described a similar phenomenon. This behavior was primarily attributed to bending or buckling failure of the ice, the rough surface, and the large angle of the ice rubble from the horizontal water level. The new ice pile was favorable for sheltering the downstream inclined structures. A continuous hill-like grounded rubble field was formed toward the sea when the ice floes had a large area. This phenomenon has been observed in previous in situ investigations in northern Bohai Sea. Fig. 12 displays a near-perfect plane below the new rubble pile, with an optimal angle of 14.1° for generating ice rubble. The angle for the ice ride-up of the broken blocks was 10.6°, which was primarily attributed to the large ice-ice friction coefficients caused by the grain structure of the blocks. Thus, the height of the ice rubble will increase for natural sea ice, which results in an enhanced sheltering effect of the IBS on the SAI.

IV. CONCLUSIONS

Tests were conducted for evaluating ice actions on an ICP and SAI protected by an IBS in shallow waters. The protective effect of the IBS on the ICP and SAI were measured in terms of the relative value of the ice load reduction and the ratio of the height of the rubble to that of the IBS, respectively. The IBS exhibited a remarkable protective effect for the ICP and SAI when the water level was lower than 0.93 times height of the IBS. Ice sheets predominately exhibited flexural failure against the IBS, which withstood considerably small cyclic horizontal forces, thus indicating the high stability of the IBS. The ice pieces hindered the ride-up of the floating ice, which primarily piled up on the IBS at a low water level. When the relative water level β was 0.16, accumulation of broken ice occurred in the upstream. With an increase in the water level, particularly for a β value higher than approximately 0.8, ice ride-up could be easily observed. The length of the broken ice fragments increased with decreasing ice loads on the IBS. The horizontal forces on the IBS and the breaking lengths increased with increasing ice thickness.

The relative ice force reduction, that is, the protective effect of the IBS on the vertical ICP (quantified using the index δ) was affected by β and the relative distance φ. When the water level was lower than the topside of the IBS, the impact forces on the ICP were considerably smaller than the ice crushing forces. A reduction of approximately 80% could be achieved in the loads of the IBS against the ICP for a β value of less than 0.8. When β was higher than 0.8, δ sharply decreased to approximately 0. By contrast, β had a more significant effect on δ than on φ.

ACKNOWLEDGMENTS

The authors are very grateful to the Key Project of Natural Science in Colleges and Universities in Anhui Province (No. KJ2015A175, No. KJ2018A0558); the Key Laboratory of Water-Sediment Sciences and Water Disaster Prevention of Hunan Province (No. 2015SS06); the Key Project of Visiting Domestic and Overseas of Outstanding Youth Core Talents of Colleges and Universities in Anhui Province (No. gxfxZD2016218); the Key Program of the National Natural Science Foundation of China (No. 51639003); the Scientific Research Fund Project of Talents of Hefei University (No. 14RC01); the Talent Research Fund Project of Hefei University (No. 16-17RC02).

REFERENCES

Barker, A. and K. Croasdale (2004). Numerical modelling of ice interaction with rubble mound berms in the Caspian Sea. Proceedings of the 17th International Symposium on Ice, Proceedings IAHR Symposium on Ice, IAHR'04, Saint Petersburg, Russia, 257-264.

Barker, A. and G. W. Timco (2005). Overview of ice rubble generators and ice protection structures in temperate regions. Proceedings of the 18th International Conference on Port and Ocean Engineering under Arctic Conditions, POAC'05, Potsdam, USA, 793-803.

Barker, A. and G. W. Timco (2016). Beaufort sea rubble fields: Characteristics and implications for nearshore petroleum operations. Cold Regions Science and Technology 121, 66-83.

Brown, T. G. and M. Määttänen (2009). Comparison of Kemi-I and Confederation Bridge cone ice load measurement results. Cold Regions Science and Technology 55(1), 3-13.

Croasdale, K. R. and A. B. Cammaert (1994). An improved method for the calculation of ice loads on sloping structures in first-year ice. Power Technology and Engineering (formerly Hydrotechnical Construction) 28(3), 174-179.

Dong, J. W., Z. J. Li, P. Lu, Q. Jia, G. Y. Wang and G. W. Li (2012). Design ice load for piles subjected to ice impact. Cold Regions Science and Technology 71, 34-43.

Evers, K. U. and A. Weihrauch (2004). Design and model testing of ice barriers for protection of offshore structures in shallow waters during winter. Proceedings of the 17th IAHR Symposium on Ice, Saint Petersburg, Russia, 21-25.

Gürtner, A. (2009). Experimental and numerical investigations of ice-structure interaction. Ph.D. thesis, Norwegian University of Science and Technology, Trondheim, Norway.

Gürtner, A. and J. Berger (2006). Results from model testing of ice protection piles in shallow water. Proceedings of the 25th International Conference on Offshore Mechanics and Arctic Engineering, Hamburg, Germany, 693-698.

Jochmann, P., K. U. Evers and W. L. Kuehnlein (2003). Model testing of ice barriers used for reduction of design ice loads. Proceedings of the 22nd International Conference on Offshore Mechanics and Arctic Engineering, Cancun, Mexico, 1-7.

Kong, X. P. and N. X. Chen (2013). Impact of the slope angle of hummocks on the ride-up of finger ice in the Liaohe Estuary. Acta Oceanologica Sinica 32(8), 12-15.

Li, G., X. Liu, Y. Liu and Q. J. Yue (2008). Optimum design of ice-resistant offshore jacket platforms in the Bohai Gulf in consideration of fatigue life of tubular joints. Ocean Engineering 35(5-6), 484-493.

Li, Z. J., G. W. Li, Y. X. Qu and Y. X. Wang (2001). Experimental Friction Coefficients Between DUT-1 Synthetic Model Ice and Materials. Proceedings of the Eleventh (2001) International Offshore and Polar Engineering Conference. Stavanger, Norway, 1, 799–802.

Li, Z. J., G. W. Li, Z. W. Shen, Y. X. Wang and Y. X. Qu (2003). Physical properties and elastic modulus of DUT-1 model ice. Journal of

Hydrodynamics, Ser. B 5, 98-102.
Li, Z., Y. X. Wang and G. W. Li (2002). On the flexural strength of DUT-1 synthetic model ice. Cold Regions Science and Technology 35(2), 67-72.
Liferov, P. (2005). Ice rubble behaviour and strength. Cold Regions Science and Technology 41(2), 153-163.
Liferov, P. and B. Bonnemaire (2005). Ice rubble behaviour and strength: Part I. Review of testing and interpretation of results. Cold Regions Science and Technology 41(2), 135-151.
Lu, W. J., R. Lubbad, K. Høyland and S. Løset (2014). Physical model and theoretical model study of level ice and wide sloping structure interactions. Cold Regions Science and Technology 101, 40-72.
Shi, W., X. Tan, Z. Gao and T. Moan (2016). Numerical study of ice-induced loads and responses of a monopile-type offshore wind turbine in parked and operating conditions. Cold Regions Science and Technology 123, 121-139.
Timco, G. W. (1990). Model Tests of Load Transmission through Grounded Ice Rubble. Journal of Offshore Mechanics and Arctic Engineering 112(2), 171-176.
Timco, G. W. and M. Johnston (2004). Ice loads on the caisson structures in the Canadian Beaufort Sea. Cold regions science and technology 38(2-3), 185-209.
Wang, S. Y., Q. J. Yue and D. Y. Zhang (2013). Ice-induced non-structure vibration reduction of jacket platforms with isolation cone system. Ocean Engineering 70, 118-123.
Wang, Y. H, X. F. Hu, Z. Q. Zhao, Q. J. Yue and N. Xu (2015). Failure mode of the ice sheet loading at the junction of the upward and downward breaking cones. Ocean Engineering 96, 34-39.
Yue, Q. J. and X. J. Bi (2000). Ice-induced jacket structure vibrations in Bohai Sea. Journal of Cold Regions Engineering 14(2), 81-92.
Zhang, D. Y. and Q. J. Yue (2011). Major challenges of offshore platforms design for shallow water oil and gas field in moderate ice conditions. Ocean Engineering 38(10), 1220-1224.